XLIII CILAMCE
21–25, November, 2022
FOZ DO IGUAÇU – PR – BRAZIL

A fem-based approach coupled to path-following strategies for non-linear anaylis of steel-concrete cross-sections

Pedro H.A. Lima[1], Ígor J.M. Lemes[2], Ricardo A.M. Silveira[1], Rafael C. Barros[3]

[1]*Dept. of Civil Engineering, Federal University of Ouro Preto*
Campus Universitário s/n, Morro do Cruzeiro, 35400-000, Ouro Preto, MG, Brazil
pedro.hal@aluno.ufop.edu.br, ricardo@ufop.edu.br
[2]*Dept. of Engineering, Federal University of Lavras*
Campus Universitário, 37200-900, Lavras, MG, Brazil
igor.lemes@ufla.br
[3]*Sereng Engineering & Consulting*
34006-056, Nova Lima, Minas Gerais, Brazil
rafaelcesario@hotmail.com

Abstract. The present study aims at the non-linear analysis of steel-concrete composite cross-sections. The strain compatibility method (SCM) is used to describe the sections deformed shape in each step of the incremental-iterative solution process. Four-node quadrilateral finite elements (FE) are implemented to compose the FE mesh of the analyzed sections. For the full analysis of the moment-curvature relationship, the SCM is coupled to path-following strategies (adapted generalized displacement technique and adapted minimum residual displacement method) to go beyond the critical bending moment points in the construction of the relations that describe the complete cross-section mechanical behavior. Concomitantly, the strain-control strategy is implemented as an alternative numerical approach and used for comparison, since the bending moment limit points do not prevent the complete construction of the cross-section equilibrium path. The constitutive relationships are addressed explicitly, as well as the residual stresses present in the steel sections. To validate the proposed numerical formulation, the results obtained are compared with the numerical and experimental data available in the literature.

Keywords: Path-following strategies, non-linear analysis, FEM, steel-concrete composite cross-sections.

1 Introduction

The analysis of cross-sectional behavior is important to measure the parameters of its stiffness and bearing capacity, directly impacting the structural element behavior. Considering the nonlinear stress-strain relationships of materials, the numerical analysis procedures must be able to accurately capture such effects.

For this evaluation, it is common to find studies that deal with the construction of interaction curves that delimit the elastic regime and the resistant capacity [1], for example. It is also possible to find analyzes of the cross-sectional behavior along the loading history through the moment-curvature relationship [2].

Bonet et al. [3] developed integration algorithms for the evaluation of reinforced concrete cross-sections subjected to biaxial bending and axial force. The decomposition of the cross-section into layers, with quadrilateral finite elements, was performed and Gauss quadrature was used to solve the integrals.Sousa Jr and Muniz [4] presented a numerical procedure for analysis of steel, reinforced concrete or composite cross-section of arbitrary polygonal shape, based on analytical evaluation of cross-section properties. The uniaxial stress–strain relationship was supposed to be of a piecewise polynomial type, and the subdivision of the section into subregions was performed by means of a contour algorithm. In a similar way, some researchers sought evaluations of the deformed state of the section for the required condition [5]. For example, Liu et al. [6] made variations in the position of the neutral axis, simultaneously considering the limiting strain of some of the cross-section component materials to analyse specific interaction curves. These studies focused in generically sections shapes or determined types, as made by Li et al. [7], that analysed rectangular tubular and welded-I cross-sections using a quasi-Newton method [8].

For the evaluation of the cross-sectional behavior after the critical point of the moment-curvature relationship, Chiorean [9] presented an incremental-iterative procedure based on arc-length approach. Thus, the active bending

moment was updated at each iterative cycle, making it possible to evaluate the cross-section with strains greater than those responsible for the critical bending moment. This approach was later applied in a brief study of a steel I section totally encased in concrete considering the AISC LRFD [10] and ECCS [11] residual stress models [12].

More recently, Lemes et al. [13, 14] used the strain compatibility method (SCM) to assess the strength and also axial and bending stiffness within the context of concentrated plasticity-based formulations. The standard Newton-Raphson method was coupled to the SCM where the constitutive relationships of the materials were explicitly used. In the these researches, a simplified incremental-iterative strategy was adopted, which was interrupted when finding the moment limit point at the moment-curvature relationship. In other words, the softening parts of these relationships were not obtained. Once using constitutive relations disregarding the materials strain-softening effect, such a softening stretch is not considered.

In this sense, Caldas [15] pointed out that a simple solution to obtain the stretches with negative rigidity of the moment-curvature relationship could be found using an increment strategy based on deformations. Chiorean [16] presented a formulation for the complete construction of the moment-curvature diagrams that were determined such that axial force and bending moment ratio was kept constant. A strain-driven algorithm was developed and implemented, and the solution of the nonlinear equilibrium equations was controlled by the assumed strain values in the most compressed point and by solving just two coupled nonlinear equations. The purpose of this work is to use path-following methods to pass through critical points in the moment-curvature relationship of cross-sections composed of steel and concrete. For corrections and control in the load increment, adaptations were made in the Generalized Stiffness Parameter (GSP) [17] to the variables present in the problem addressed here. During the iterative process, the minimum residual displacement norm strategy [18] was adapted.

2 Materials constitutive relationships

The behavior of the steel will be described through the trilinear constitutive model [12] depicted in Fig. 1. It should be emphasized that the possibility of the material hardening is considered. One characteristic of steel section material is that its tensile behavior equals that of compression.

For steel reinforcement, a bilinear constitutive relationship was considered according [12]. This model was adopted for both tension and compression, in which the strain-hardening effect was considered only in tension.

Compressed concrete is described by the nonlinear relation [12] and when tensioned, the bilinear constitutive model, with the maximum tensile strain limited to 0.07% [19], was used.

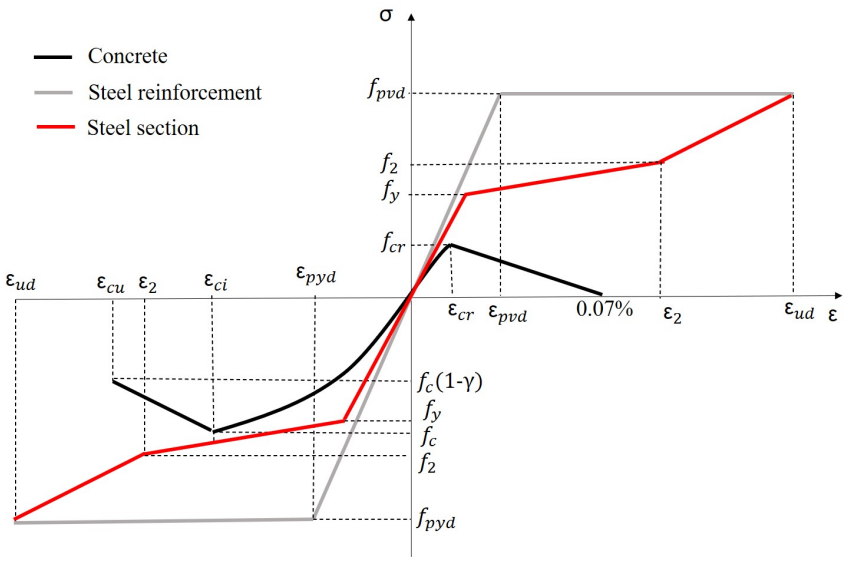

Figure 1. Constitutive relationships adopted for the materials

The residual stress models used in this research are defined by design codes. The ECCS [11] uses the residual stress model based on Huber and Beedle's [20] proposition. AISC LRFD [10] follows the Galambos and Ketter [21] proposal.

3 Cross-sectional analysis

The SCM is an Euler-Bernoulli Theory-based approach for the evaluation of compact cross-sections. Under external loads, a structure will gradually deform until it reaches equilibrium [10]. Once the internal and external forces are equal, the deformation stops, and, at the cross-section level, is studied by SCM [13].

3.1 Degrees of freedom

The discretization shown in Figure 5 is used to find the axial strain, ε_i , in plastic centroid (PC) of each cross-sectional sub-area. Thus, through the material constitutive relationship, it is possible to obtain the respective stress, σ_i. In Figure 5, the deformed shape of an I section is illustrated for a combination of normal efforts (axial force and bending moment). Thus, the axial strain in the i^{th} sub-area can be written as follows:

$$\varepsilon_i = \varepsilon_0 + \Phi y_i + \varepsilon_{ri} \tag{1}$$

where y_i is the distance between the plastic centroids of the analyzed sub-area and the cross section, ε_0 is the axial strain of the PC section, ε_r is the strain due to residual stress, and Φ is its curvature. The variables ε_0 and Φ are the strain vector components.

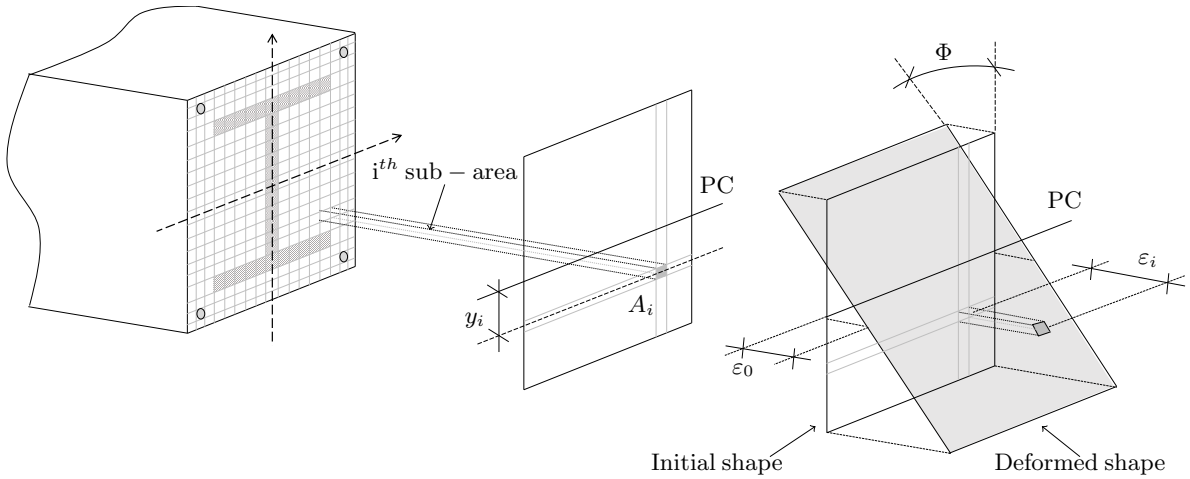

Figure 2. Linear strain field in major axis bending

The internal force vector for this case is expressed by the classical integrations (summations) and considering the cross-sectional discretization, as follows:

$$\mathbf{f}_{int} = \begin{bmatrix} N_{int} = \displaystyle\int_A \sigma\left[\varepsilon\left(\varepsilon_0, \Phi\right)\right] dA \\ M_{int} = \displaystyle\int_A \sigma\left[\varepsilon\left(\varepsilon_0, \Phi\right)\right] y dA \end{bmatrix} = \begin{bmatrix} N_{int} = \displaystyle\sum_{i=1}^{n_{sub}} \sigma_i\left[\varepsilon_i\left(\varepsilon_0, \Phi\right)\right] A_i \\ M_{int} = \displaystyle\sum_{i=1}^{n_{sub}} \sigma_i\left[\varepsilon_i\left(\varepsilon_0, \Phi\right)\right] y_i A_i \end{bmatrix} \tag{2}$$

where N_{int} and M_{int} are the internal forces.

3.2 Constitutive matrix

The cross-section discretization shown in Figure 2 is very efficient [22] in describing the strain distribution. It is done to capture the axial strain in the center of each sub-area, and then (through the material constitutive relations) to obtain the respective stresses. Thus, the axial stress in i_{th} sub-area can be obtained by the Eq.(1).

The cross-sectional deformed shape is calculated by the equilibrium of the external, $\mathbf{f}_{ext}$, and internal, $\mathbf{f}_{int}$, forces that can be numerically expressed by the following nonlinear equation:

$$\mathbf{F}\left(\mathbf{X}\right) = \mathbf{f}_{ext} - \mathbf{f}_{int} \cong 0 \tag{3}$$

with $\mathbf{F}$ and $\mathbf{X}$ being the equilibrium force vector and strain vector, respectively. All parameters are dependent

of the number of degrees of freedom of the section. Applying the expansion in Taylor series in Eq.(3), results in the following set of nonlinear equations:

$$\mathbf{F(X)} = \mathbf{F'(X)}\Delta\mathbf{X} \tag{4}$$

where $\mathbf{F'}$ is the Jacobian matrix of the nonlinear problem, that is described as follow:

$$\mathbf{F'(X)} = -\frac{\partial \mathbf{F(X)}}{\partial \mathbf{X}} = \begin{bmatrix} f_{11} = \dfrac{\partial N_{int}}{\partial \varepsilon_0} & f_{12} = \dfrac{\partial N_{int}}{\partial \Phi} \\ f_{21} = \dfrac{\partial M_{int}}{\partial \varepsilon_0} & f_{22} = \dfrac{\partial M_{int}}{\partial \Phi} \end{bmatrix} \tag{5}$$

3.3 Generalized stiffness parameters

When the cross-section equilibrium is reached, the external and internal forces vectors are numerically equal. Thus, the deformed shape of the cross-section, described by strain vector **X**, is found. For this condition, the parameters of cross-sectional stiffness are determined. In turn, the axial strains in the sub-areas are used to calculate the Jacobian matrix at this point, where:

$$\begin{bmatrix} f_{11} & f_{12} \\ f_{21} & f_{22} \end{bmatrix} \begin{Bmatrix} \Delta\varepsilon \\ \Delta\Phi \end{Bmatrix} = \begin{Bmatrix} \Delta N \\ \Delta M \end{Bmatrix} \tag{6}$$

Using the stiffness concept, the differentiation of the force by its respective strain defines the stiffness of the analysed degree of freedom. As the problem has two degrees of freedom, to obtain the axial stiffness the bending moment is kept constant ($\Delta M = 0$). Therefore, the system resolution to obtain the ratio of the force increment ΔN by the axial strain increment $\Delta\varepsilon$ defines the section axial stiffness EA_T. The same process can be adapted to obtain flexural stiffness EI_T. The calculated stiffnesses are presented below:

$$EA_T = \left.\frac{\Delta N}{\Delta\varepsilon}\right|_{\Delta M=0} = f_{11} - \frac{f_{12}f_{21}}{f_{22}} \tag{7}$$

$$EI_T = \left.\frac{\Delta M}{\Delta\Phi}\right|_{\Delta N=0} = f_{22} - \frac{f_{12}f_{21}}{f_{11}} \tag{8}$$

where f_{ij} are the constitutive matrix terms defined by Eq. (5)

4 Path-following strategies

In finite element context, the nonlinear static solver consists of obtaining the equilibrium between internal and external forces for each load increment as described in Eq. (3) and modified as follows [14]:

$$\mathbf{f}_{ext} - \mathbf{f}_{int} \cong 0 \rightarrow \underbrace{(\mathbf{f}_{fix} + \lambda\mathbf{f}_r)}_{\mathbf{f}_{ext}} - \mathbf{f}_{int} \cong 0 \tag{9}$$

where $\mathbf{f}_{fix}$ is fixed forces vector, λ is the bending moment increment factor and $\mathbf{f}_r$ is the reference load vector.

To solve the nonlinear problem, load increment and iteration strategies are used.

The initial increase of the load parameter, $\Delta\lambda^0$, is automatically determined by the modified technique of generalized displacement [23]. Thus, $\Delta\lambda^0$ is calculated as:

$$\Delta\lambda^0 = \pm\Delta\lambda_1^0\sqrt{\left|\frac{\left({}^1\delta\mathbf{X}_r^T\right)\left({}^1\delta\mathbf{X}_r\right)}{\left({}^t\delta\mathbf{X}_r^T\right)\left(\delta\mathbf{X}_r\right)}\right|} = \pm\Delta\lambda_1^0\sqrt{|GSP|} \tag{10}$$

where index 1 indicates the $\Delta\lambda^0$ and $\delta\mathbf{X}_r$ (tangential strains) values obtained in the first loading step, and GSP represents the Generalized Stiffness Parameter.

In the traditional scheme of the Newton-Raphson method, the load parameter λ is kept constant throughout the iterative process. Thus, the equilibrium path can be obtained until a limit point and/or a bifurcation point is reached. The variation of λ during the iterative cycle enables the full equilibrium path to be traced. In this work,

the minimum residual displacement norm strategy proposed by Chan [18] was used. In this strategy, the correction of the load parameter $\delta\lambda^k$ is given by the equation:

$$\delta\lambda^k = -\frac{\left(\delta\mathbf{X}_r^k\right)^T \delta\mathbf{X}_g^k}{\left(\delta\mathbf{X}_r^k\right)^T \delta\mathbf{X}_r^k} \tag{11}$$

where $\delta\mathbf{X}_g^k$ is the displacement vector correction obtained from the Newton-Raphson method application with the conventional λ increment strategy, and $\delta\mathbf{X}_r^k$ is the iterative displacement vector resulting from reference load vector $\mathbf{f}_r$ application.

5 Moment-curvature relationship

In this work, the standard Newton-Raphson method and continuation strategy were used to obtain the moment-curvature relationship. For a fixed value of axial force, N, increments are given in the external bending moment, M, until the ultimate strain of one of the materials is reached. The process of the moment-curvature relationship assessment can be seen in Figure 3:

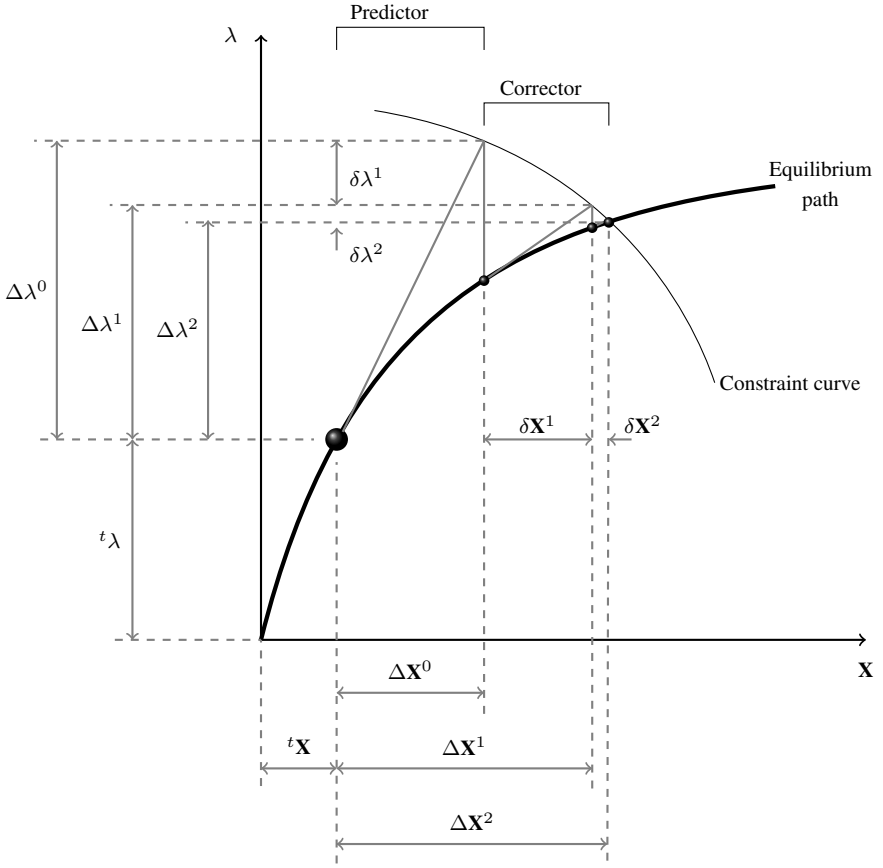

Figure 3. Numerical strategy adopted for the iterative-incremental solution

Table 1 sequentially describes the nonlinear solver adopted for the cross-sectional problem considering ith the axial strain of the ith subarea and ε_{lim} the material ultimate strain of the analysed subarea.

Table 1. Flowchart of the moment-curvature relationship assessment

	Algotithm: Nonlinear solver
1	Read geometric and material data of the cross-section
2	Obtain the reference nodal load vector, $\mathbf{F}_r$
3	$t = 0$
4	$t_1 = t$
5	Initial conditions: ${}^t\mathbf{X} = 0$ and ${}^t\lambda = 0$
6	**for** each load increment **do** $\rightarrow$ **INCREMENTAL PROCESS**
7	$t = t_1 \rightarrow$ Previous load step
8	$t_1 = t + 1 \rightarrow$ Current load step
9	Assemble the constitutive matrix: **F'**
10	Solve: tangent displacement vector: $\delta\mathbf{X}_r$ = $\mathbf{F}'^{-1}\,\mathbf{F}_r$
11	**if** $t_1 = 1$ **then**
12	$\Delta\lambda^0 = (\Delta\lambda^0)_1$
13	**else**
14	Define: $\Delta\lambda^0 (Eq.10)$
15	**end if**
16	Evaluate the initial incremental strain vector: $\Delta\mathbf{X}^0 = \Delta\lambda^0\delta\mathbf{X}_r$
17	Update variables in t_1: ${}^{t1}\lambda = {}^t\lambda + \Delta\lambda^0 and {}^{t1}\mathbf{X} = {}^t\mathbf{X} + \Delta\mathbf{X}^0$
18	**for** $k = 1$, *nmax* **do** $\rightarrow$ **ITERATIVE PROCESS**
19	Evaluate the internal forces vector: ${}^{t1}\mathbf{f}_{int}^{(k-1)}$
20	Evaluate the residual force vector: $\mathbf{g}^{(k-1)} = (\mathbf{f}_{fix} + {}^{t1}\,\lambda^{(k-1)}\mathbf{F}_r) - {}^{t1}\,\mathbf{f}_{int}^{(k-1)}$
21	**if** $\varsigma \leq Tol$ **then**
22	Exit the iterative process and go to line 30
23	**end if**
24	Update the constitutive matrix **F'**
25	Update the load parameter correction, $\lambda^k (Eq.11)$
26	Evaluate the strain correction vector: $\delta\mathbf{X}^k = \delta\mathbf{X}_g^k + \delta\lambda^k\delta\mathbf{X}_r^k$
27	Update the load parameter and the strain vector: $\Delta\lambda^k = \Delta\lambda^{(k-1)} + \delta\lambda^k and \Delta\mathbf{X}^k = \Delta\mathbf{X}^{(k-1)} + \delta\mathbf{X}_g^k + \delta\lambda^k\delta\mathbf{X}_r^k$ ${}^{t1}\lambda^k = {}^t\lambda + \Delta\lambda^k and {}^{t1}\mathbf{X}^k = {}^t\mathbf{X} + \Delta\mathbf{X}^k$
28	**end for**
29	Update the variables (strains and internal forces vector)
30	**if** $(\varepsilon_i > \varepsilon_{lim})$**then**
31	Stop
32	**end if**
33	**end for**

6 Numerical applications

7 Conclusions

Acknowledgements. The authors would like to thank CAPES and CNPq (Federal Research Agencies), Fapemig (Minas Gerais State Research Agency), UFLA and UFOP for their support during the development of this work.

Authorship statement. The authors hereby confirm that they are the sole liable persons responsible for the au-

thorship of this work, and that all material that has been herein included as part of the present paper is either the property (and authorship) of the authors, or has the permission of the owners to be included here.

References

[1] Í. J. M. Lemes, A. R. D. Silva, R. A. M. Silveira, and P. A. S. Rocha. Numerical analysis of nonlinear behavior of steel concreto composite structures. *Ibracon Structures and Materials Journal*, vol. 10, n. 1, pp. 53–83, 2017b.

[2] Í. J. M. Lemes, A. R. D. Silva, R. A. M. Silveira, and P. A. S. Rocha. Determinação da capacidade resistente de elementos estruturais mistos através do método da rótula plástica refinado. *Revista Internacional de Métodos Numéricos para Cálculo y Diseño en Ingeniería*, vol. 33, n. 1-2, pp. 24–34, 2017a.

[3] J. L. Bonet, M. Romero, P. Miguel, and M. Fernandez. A fast stress integration algorithm for reinforced concrete sections with axial loads and biaxial bending. *Computers Structures*, vol. 82, pp. 213–225, 2004.

[4] J. B. M. Sousa Jr and C. F. D. G. Muniz. Analytical integration of cross section properties for numerical analysis of reinforced concrete, steel and composite frames. *Engineering Structures*, vol. 29, n. 4, pp. 618–625, 2007.

[5] M. Fong and S. L. Chan. Advanced analysis of steel-concrete composite beam-columns by refined plastic-hinge method. *International Journal of Structural Stability and Dynamics*, vol. 12, n. 6, 2012.

[6] S. W. Liu, Y. P. Liu, and S. L. Chan. Advanced analysis of hybrid steel and concrete frames part 1: Cross-section analysis technique and second-order analysis. *Journal of Constructional Steel Research*, vol. 70, pp. 326–336, 2012a.

[7] T. Li, S. Liu, and S. Chan. Direct analysis for high-strength steel frames with explicit model of residual stresses. *Engineering Structures*, vol. 100, pp. 342–355, 2015.

[8] S. Chen, J. G. Teng, and S. L. Chan. Design of biaxially loaded short composite columns of arbitrary section. *Journal of Structural Engineering*, vol. 127, n. 6, pp. 678–685, 2001.

[9] C. Chiorean. Computerised interaction diagrams and moment capacity contours for composite steel–concrete cross-sections. *Engineering Structures*, vol. 32, n. 11, pp. 3734–3757, 2010.

[10] AISC LRFD. Specification for structural steel buildings. *American Institute of Steel Construction, Chicago, IL*, 2016.

[11] ECCS. Ultimate limit state calculation of sway frames with rigid joints. *European Convention for Constructional Steelwork. Technical Committee 8. Structural Stability. Technical Working Group 8.2. System*, 1984.

[12] C. G. Chiorean. A computer method for nonlinear inelastic analysis of 3D composite steel-concrete frame structures. *Engineering Structures*, vol. 57, pp. 125–152, 2013.

[13] Í. J. M. Lemes, R. A. M. Silveira, A. R. D. Silva, and P. A. S. Rocha. Nonlinear analysis of two-dimensional steel, reinforced concrete and composite steel-concrete structures via coupling SCM/RPHM. *Engineering Structures*, vol. 147, pp. 12–26, 2017.

[14] Í. J. M. Lemes, R. C. Barros, R. A. M. Silveira, A. R. D. Silva, and P. A. S. Rocha. Numerical analysis of rc plane structures: a concentrated nonlinear effect approach. *Latin American Journal of Solids and Structures*, vol. 15, n. 2, 2018.

[15] R. B. Caldas. Análise numérica de pilares mistos aço-concreto. Master's thesis, Programa de Pós Graduação em Engenharia Civil, Universidade Federal de Ouro Preto, Ouro Preto, MG, Brasil, 2004.

[16] C. Chiorean. A computer method for moment-curvature analysis of composite steel-concrete cross-sections of arbitrary shape. *Engineering Structures and Technologies*, vol. 9, n. 1, pp. 25–40, 2017.

[17] Y. Yang and S. Kuo. *Theory & analysis of nonlinear framed structures*. Prentice Hall, 1994a.

[18] S. L. Chan. Geometric and material non-linear analysis of beam-columns and frames using the minimum residual displacement method. *International Journal of Numerical Methods in Engineering*, vol. 26, n. 12, pp. 2657–2669, 1988.

[19] S. Bratina, M. Saje, and I. Planinc. On material and geometrically non-linear analysis of reinforced concrete planar frames. *International Journal of Solids and Structures*, vol. 41, pp. 7181–7207, 2004.

[20] A. W. E. Huber and L. S. Beedle. Residual stress and the compressive strength of steel. *Welding Journal*, vol. 33, pp. 589–614, 1954.

[21] T. Galambos and R. Ketter. Columns under combined bending and thrust. *Journal of the Engineering Mechanics Division*, vol. 85, pp. 1–30, 1959.

[22] Í. J. M. Lemes, L. E. S. Dias, R. A. M. Silveira, A. R. Silva, and T. A. Carvalho. Numerical analysis of steel–concrete composite beams with partial interaction: A plastic-hinge approach. *Engineering Structures*, vol. 248, pp. 113256, 2021.

[23] Y.-B. Yang and S.-R. Kuo. *Theory and analysis of nonlinear framed structures*. Prentice Hall PTR, 1994b.